Spatiotemporal electromagnetic soliton and spatial ring formation in nonlinear metamaterials

Jinggui Zhang, Shuangchun Wen,* Yuanjiang Xiang, Youwen Wang, and Hailu Luo

Key Laboratory for Micro/Nano Optoelectronic Devices of Ministry of Education, School of Computer and Communication, Hunan University, Changsha 410082, People's Republic of China

(Received 8 October 2009; published 24 February 2010)

We present a systematic investigation of ultrashort electromagnetic pulse propagation in metamaterials (MMs) with simultaneous cubic electric and magnetic nonlinearity. We predict that spatiotemporal electromagnetic solitons may exist in the positive-index region of a MM with focusing nonlinearity and anomalous group velocity dispersion (GVD), as well as in the negative-index region of the MM with defocusing nonlinearity and normal GVD. The experimental circumstances for generating and manipulating spatiotemporal electromagnetic solitons can be created by elaborating appropriate MMs. In addition, we find that, in the negative-index region of a MM, a spatial ring may be formed as the electromagnetic pulse propagates for focusing nonlinearity and anomalous GVD; while the phenomenon of temporal splitting of the electromagnetic pulse may appear for the same case except for the defocusing nonlinearity. Finally, we demonstrate that the nonlinear magnetization makes the sign of effective electric nonlinear effect switchable due to the combined action of electric and magnetic nonlinearity, exerting a significant influence on the propagation of electromagnetic pulses.

DOI: 10.1103/PhysRevA.81.023829 PACS number(s): 42.65.Tg, 42.65.Sf

I. INTRODUCTION

The underlying physical mechanism for ultrashort electromagnetic pulse propagation in conventional nonlinear materials has been well understood [1,2]. Generally speaking, different qualitative spatiotemporal dynamical behaviors of pulse evolution may occur, completely depending on the interplay of dispersion, diffraction, and nonlinear processes. In anomalous group velocity dispersion (GVD), Silberberg theoretically predicted that the cubic self-focusing nonlinearity can compensate for both diffraction and dispersion simultaneously, resulting in the formation of nondispersing and nodiffracting pulses, namely, spatiotemporal solitons, sometimes called "light bullets" to convey their particle-like nature, when diffraction and dispersion have the same magnitude [3]. However, a small perturbation will lead to collapse of such a multidimensional soliton in a cubic medium. Nevertheless, several ways to arrest the collapse and stabilize spatiotemporal soliton have been proposed [1]. The experimental realization of three-dimensional spatiotemporal solitons in a cubic medium still poses significant challenges to researchers owing to the difficulty of creating appropriate experimental conditions [1–4]. In the normal GVD, previous theoretical and experimental results demonstrated that, above a certain threshold power, the light pulse in a cubic medium may undergo temporal splitting which can arrest catastrophic self-focusing [5,6]; while spatial ring formation may occur in a saturating nonlinear optical medium [7].

Recently, artificially designed and engineered materials, namely the metamaterials (MMs), have aroused increasing interest in the scientific community due to their intriguing properties, which are unattainable in naturally occurring materials, and a variety of unprecedented applications [8–11]. Advances in the fabrication of MMs, ranging from microwave to optical frequency [9–14] and from linear to nonlinear [15–17], has further stimulated a great deal of research, including the revaluation and characterization of the classical nonlinear optical processes. It is known that MMs have rich and unusual linear and nonlinear electromagnetic properties, indicating that MMs may be a new but important candidate for solitons and other nonlinear optical phenomena such as ultrashort electromagnetic pulse propagation [18–25]. In addition, both linear and nonlinear electromagnetic properties of MMs are engineerable, thus the manipulation of electromagnetic or light waves in MMs will be more desirable. Since 2005, some dynamical models for describing ultrashort pulse propagation in MMs with a cubic nonlinear polarization and/or a nonlinear magnetization have been established [18–22], several intriguing and counterintuitive nonlinear phenomena associated with pulse propagation and modulation instability have been disclosed [18–25], and various soliton phenomena and physics have been demonstrated [18–22,26–34].

In this paper, we present a systematic investigation of electromagnetic pulse propagation in MMs with both cubic electric and cubic magnetic nonlinearity, focusing on the unusual propagation properties of electromagnetic pulses associated with the unique electromagnetic properties of the MMs. As is well known, the evolution of spatiotemporal electromagnetic pulses is mainly governed by the interplay among dispersion, diffraction, and nonlinearity in a dispersive nonlinear medium. For MMs described by the Drude model, diffraction may be either positive or negative, depending on the sign of the refractive index seen by the propagating pulse in MMs [19,20]. This provides us with more combinations for the signs of dispersion, diffraction, and nonlinearity, greatly enriching the dynamical behaviors of electromagnetic pulse propagation. We will show that the MMs can be exploited to create appropriate experimental circumstances for generating and manipulating spatiotemporal electromagnetic solitons. We will also predict the counterintuitive conditions for the interesting phenomena of spatial ring formation and temporal splitting of pulsed electromagnetic beams in MMs and elucidate the underlying physical mechanisms. Moreover, we will discuss the role of the additional nonlinear magnetization

*scwen@hnu.cn

[18–21], which has never arisen in conventional materials, in the propagation of electromagnetic pulses. We find that the nonlinear magnetization makes the sign of the effective electric nonlinear effect switchable due to the combined action of electric and magnetic nonlinearity, exerting a significant influence on the propagation of electromagnetic pulses.

The rest of this paper has been split into several parts. In Sec. II we present the basic propagation models for ultrashort pulse propagation in MMs with a cubic nonlinear polarization and/or a nonlinear magnetization and discuss the linear and nonlinear properties of the MMs described by the Drude model. In Sec. III, first, by utilizing the variational approach we arrive at an explicit, although approximate, analytical spatiotemporal soliton solution and analyze the requirements for the existence of spatiotemporal electromagnetic solitons in bulk MMs. Then, based on the split-step Fourier method, we investigate the physical mechanism for spatial ring formation and temporal splitting of electromagnetic pulses. Finally, we discuss the controllable sign of the nonlinear effect in MMs and its role in the propagation of electromagnetic pulses. A brief conclusion will be given in Sec. IV.

II. NONLINEAR PROPAGATION MODELS FOR SPATIOTEMPORAL ELECTROMAGNETIC PULSES IN METAMATERIALS

A MM usually shows a microscopic periodic structure [9,15]. When the characteristic scale of the wavelength of the electromagnetic field is much larger than the period of the microstructured medium, the effective medium approach for both linear and nonlinear MMs is applicable. In such an approach, a microstructured composite is treated as a homogeneous isotropic medium characterized by an effective electric permittivity $\varepsilon(\omega)$ and magnetic permeability $\mu(\omega)$, which are strongly affected by the internal structure of the medium [15–25]. We consider electromagnetic pulse propagation in this regime, and thus we can assume that the pulse is propagating in uniform, bulk material, in which there are no free charges and in which no free currents flow. In addition, we assume the MM has a nonlinear electric polarization and a nonlinear magnetization. Taking into full consideration the unique characteristics of the MM, one can obtain the following coupled nonlinear Schrödinger equations (NLSEs) describing nonlinear propagation of ultrashort electromagnetic pulses in MMs by following the classical steps for deducing NLSEs in ordinary dielectrics [20]:

$$\frac{\partial E}{\partial \xi} = -\frac{i\beta_2}{2}\frac{\partial^2 E}{\partial \tau^2} + \frac{i}{2\beta_0}\nabla_\perp^2 E + \frac{i\eta\omega_0\varepsilon_0\chi_p^{(3)}}{2}|E|^2E + \frac{i\omega_0\mu_0\chi_m^{(3)}}{2}|H|^2H, \tag{1a}$$

$$\frac{\partial H}{\partial \xi} = -\frac{i\beta_2}{2}\frac{\partial^2 H}{\partial \tau^2} + \frac{i}{2\beta_0}\nabla_\perp^2 H + \frac{i\omega_0\mu_0\chi_m^{(3)}}{2\eta}|H|^2H + \frac{i\omega_0\varepsilon_0\chi_p^{(3)}}{2}|E|^2E, \tag{1b}$$

where E and H are the envelope amplitudes of electric and magnetic fields, respectively, ξ is the propagation distance, τ is time in the co-moving reference frame, $\nabla_\perp^2 = \partial^2/\partial x^2 + \partial^2/\partial y^2$ is the transverse Laplace operator, ε_0 and μ_0 are, respectively, the electric permittivity and the magnetic permeability in vacuum, ω_0 is the carrier frequency of the electromagnetic pulse, β_0 is the corresponding wave number in MMs, β_2 accounts for group-velocity dispersion, $\chi_p^{(3)}$ and $\chi_m^{(3)}$ are, respectively, the third-order electric and magnetic susceptibilities, and $\eta = \eta_0\eta_r \equiv \sqrt{\mu_0/\varepsilon_0}\sqrt{\mu_r/\varepsilon_r}$ is the impedance of MMs, where η_0 and η_r are the impedance in vacuum and the relative impedance of the medium, respectively, and ε_r and μ_r are the relative electric permittivity and relative magnetic permeability, respectively. It should be noted that, in the derivation of the set of Eqs. (1), we have assumed a Kerr-type nonlinear polarization $P_{\mathrm{NL}} = \varepsilon_0\chi_p^{(3)}|E|^2E$ and a Kerr-type nonlinear magnetization $M_{\mathrm{NL}} = \mu_0\chi_m^{(3)}|H|^2H$. For a MM created by arrays of wires and split-ring resonators embedded in a nonlinear Kerr dielectric [15], such a material has a Kerr-type nonlinear polarization and a comparatively complicated form of nonlinear magnetization, similar to the form of saturation nonlinearity. However, for a relatively small magnetic field intensity, the nonlinear magnetization can also be taken as the Kerr type [18,28]. In addition, the higher order linear dispersion terms and higher order nonlinear terms have been neglected in this paper for simplicity.

Obviously, the equations for the electric field [Eq. (1a)] and the magnetic field [Eq. (1b)] exhibit an evident symmetry; in fact we can formally obtain Eq. (1b) from Eq. (1a) and vice versa with the formal substitutions $\varepsilon_0 \to \mu_0$, $\mu_0 \to \varepsilon_0$, $E \to H$, and $H \to E$. Further, the coupled system (1) can be incorporated into a single equation for the electric field by using the relation between magnetic and electric fields [20]:

$$H = \frac{-i}{\omega_0\mu_0\left(\mu_r + \chi_m^{(3)}|H|^2\right)}\left(\frac{\partial E}{\partial \xi} + i\beta_0 E\right). \tag{2}$$

Under the slowly varying envelope approximation ($|\partial E/\partial\xi| \ll |\beta_0 E|$) and the approximation $|\chi_m^{(3)}||H|^2 \ll |\mu_r|$, we have $H \approx E/\eta$. Substituting this relation into Eq. (1a) we obtain

$$\frac{\partial E}{\partial \xi} = -\frac{i\beta_2}{2}\frac{\partial^2 E}{\partial \tau^2} + \frac{i}{2\beta_0}\nabla_\perp^2 E + \frac{i\eta\omega_0\varepsilon_0\chi_p^{(3)}}{2}\left(1 + \frac{\mu_0\chi_m^{(3)}}{\eta^4\varepsilon_0\chi_p^{(3)}}\right)|E|^2E. \tag{3}$$

For convenience of computation, we define four characteristic lengths for diffraction, dispersion, and electric and magnetic nonlinearity, respectively, as follows:

$$L_{\mathrm{DF}} = \left|\beta_0 w_0^2\right|, \tag{4a}$$

$$L_{\mathrm{DS}} = \left|\frac{\tau_0^2}{\beta_2}\right|, \tag{4b}$$

$$L_{\mathrm{ENL}} = \frac{2}{\omega_0\varepsilon_0\eta\left|\chi_p^{(3)}\right||E_0|^2}, \tag{4c}$$

$$L_{\mathrm{HNL}} = \frac{2\eta}{\omega_0\mu_0\left|\chi_m^{(3)}\right||H_0|^2}, \tag{4d}$$

where w_0 is the initial input beam radius ($1/e$) and τ_0 is the initial pulse width ($1/e$), and E_0 and H_0 are the initial amplitudes of the electric and magnetic field envelopes, respectively. Now

we normalize Eq. (3) using the transformations $Z = \xi/L_{\mathrm{DF}}$, $X = x/w_0$, $Y = y/w_0$, $T = \tau/\tau_0$, and $A = E/E_0$:

$$\frac{\partial A}{\partial Z} = -\frac{i\,\mathrm{sgn}\,(\beta_2)}{2} s \frac{\partial^2 A}{\partial T^2} + \frac{i\,\mathrm{sgn}\,(n)}{2}\nabla_\perp^2 A + ip|A|^2 A, \qquad (5)$$

where $\mathrm{sgn}\,(\beta_2) = \pm 1$ corresponds to normal and anomalous GVD, respectively, and $\mathrm{sgn}\,(n) = \pm 1$ corresponds to positive-index and negative-index material, respectively. The dimensionless dispersion coefficient is $s = L_{\mathrm{DF}}/L_{\mathrm{DS}}$, and the nonlinear coefficient p in Eq. (5) is given by

$$p = \mathrm{sgn}\left(\chi_p^{(3)}\right)\frac{L_{\mathrm{DF}}}{L_{\mathrm{ENL}}}\left[1 + \mathrm{sgn}\left(\chi_m^{(3)}/\chi_p^{(3)}\right)\frac{L_{\mathrm{ENL}}}{f^2 L_{\mathrm{HNL}}}\right], \qquad (6)$$

where $f = \eta H_0/E_0 \approx 1$ because $H \approx E/\eta$. Here $\mathrm{sgn}\,(\chi_p^{(3)}) = \pm 1$ stands for focusing and defocusing electric nonlinearity, respectively, and $\mathrm{sgn}\,(\chi_m^{(3)}) = \pm 1$ stands for focusing and defocusing magnetic nonlinearity, respectively. Obviously, the parameter p can be positive or negative, and its sign is dependent on the combined effect of electric and magnetic nonlinearity. In this paper, $\mathrm{sgn}\,(p) = \pm 1$ is considered as the focusing and defocusing nonlinearity for MMs, respectively, as in conventional materials. In what follows, we will investigate the generic propagation properties of electromagnetic pulses in MMs based on Eq. (5).

The properties of MMs are described by the Drude model in the paper, in which the relative permittivity and relative magnetic permeability are expressed as

$$\varepsilon_r(\omega) = 1 - \frac{\omega_{\mathrm{pe}}^2}{\omega^2},\ \mu_r(\omega) = 1 - \frac{\omega_{\mathrm{pm}}^2}{\omega^2}, \qquad (7)$$

where ω_{pe} and ω_{pm} are the electric and magnetic plasma frequencies. Here for simplicity we have neglected the electric and magnetic losses in the following analysis. From Eq. (7) we can easily obtain the expressions for the refractive index n, relative impedance η_r, and GVD β_2:

$$n = \pm\sqrt{\left(1 - \frac{\omega_{\mathrm{pe}}^2}{\omega^2}\right)\left(1 - \frac{\omega_{\mathrm{pm}}^2}{\omega^2}\right)}, \qquad (8a)$$

$$\eta_r = \sqrt{\frac{\omega^2 - \omega_{\mathrm{pm}}^2}{\omega^2 - \omega_{\mathrm{pe}}^2}}, \qquad (8b)$$

$$\beta_2 = \frac{\Gamma}{c\omega_{\mathrm{pe}}}, \qquad (8c)$$

where $\Gamma = \omega_{\mathrm{pe}}(1 + 3\omega_{\mathrm{pe}}^2\omega_{\mathrm{pm}}^2\omega^{-4})/n\omega - \omega_{\mathrm{pe}}(1 - \omega_{\mathrm{pe}}^2\omega_{\mathrm{pm}}^2\omega^{-4})^2/n^3\omega$. Based on the Drude model, the corresponding diffraction length, dispersion length, and nonlinear lengths for electric and magnetic fields, respectively, can be transformed into the following forms:

$$L_{\mathrm{DF}} = L_{\mathrm{DF}}^0\left|\frac{n\omega}{\omega_{\mathrm{pe}}}\right|, \qquad (9a)$$

$$L_{\mathrm{DS}} = \frac{L_{\mathrm{DS}}^0}{|\Gamma|}, \qquad (9b)$$

$$L_{\mathrm{ENL}} = \frac{L_{\mathrm{ENL}}^0\omega}{\omega_{\mathrm{pe}}\eta_r}, \qquad (9c)$$

$$L_{\mathrm{HNL}} = \frac{L_{\mathrm{HNL}}^0\eta_r\omega}{\omega_{\mathrm{pe}}}, \qquad (9d)$$

where

$$L_{\mathrm{DF}}^0 = \frac{\omega_{\mathrm{pe}} w_0^2}{c}, \qquad (10a)$$

$$L_{\mathrm{DS}}^0 = c\tau_0^2\omega_{\mathrm{pe}}, \qquad (10b)$$

$$L_{\mathrm{ENL}}^0 = \frac{2}{\eta_0\omega_{\mathrm{pe}}\varepsilon_0\left|\chi_p^{(3)}\right||E_0|^2}, \qquad (10c)$$

$$L_{\mathrm{HNL}}^0 = \frac{2\eta_0}{\mu_0\omega_{\mathrm{pe}}\left|\chi_m^{(3)}\right||H_0|^2}, \qquad (10d)$$

and where c is the light velocity in vacuum.

The linear and nonlinear properties of MMs described by the Drude model are summarized in Fig. 1. The left-hand column shows the four characteristic lengths L_{DF}, L_{DS}, L_{ENL}, and L_{HNL} versus normalized frequency $\omega/\omega_{\mathrm{pe}}$, and the right-hand column shows n, η_r, and β_2 versus $\omega/\omega_{\mathrm{pe}}$. We clearly see that, for the Drude model, the electromagnetic MM exhibits quite different properties in the three regions. (1) In the negative-index region [$\mathrm{sgn}\,(n) < 0$], β_2 can be either positive or negative in the case of $\omega_{\mathrm{pm}}/\omega_{\mathrm{pe}} > 1$ or $\omega_{\mathrm{pm}}/\omega_{\mathrm{pe}} <$; while β_2 is always negative in the case of $\omega_{\mathrm{pe}}/\omega_{\mathrm{pm}} = 1$. (2) In the stop-band region (gray region), no incident electromagnetic wave can propagate. (3) In the positive-index region [$\mathrm{sgn}\,(n) > 0$], β_2 is always negative. For simplicity of discussion, we assume that $L_{\mathrm{ENL}}^0 = L_{\mathrm{HNL}}^0$ and $L_{\mathrm{DS}}^0 = L_{\mathrm{DF}}^0$ in the following analysis. Under such conditions, some interesting conclusions about the four characteristic lengths can be drawn from Fig. 1. First, when $\omega_{\mathrm{pm}}/\omega_{\mathrm{pe}} < 1$ and $\mathrm{sgn}\,(n) < 0$, or when $\omega_{\mathrm{pm}}/\omega_{\mathrm{pe}} > 1$ and $\mathrm{sgn}\,(n) > 0$, the electric nonlinear length L_{ENL} is always longer than the magnetic nonlinear length L_{HNL}, and near the plasma frequency, L_{ENL} tends to become very long while L_{HNL} tends to become very short. When $\omega_{\mathrm{pm}}/\omega_{\mathrm{pe}} > 1$ and $\mathrm{sgn}\,(n) < 0$, or when $\omega_{\mathrm{pm}}/\omega_{\mathrm{pe}} < 1$ and $\mathrm{sgn}\,(n) > 0$, the electric nonlinear length L_{ENL} is always shorter than the magnetic nonlinear length L_{HNL}, and near the plasma frequency, L_{ENL} tends to become very short while L_{HNL} tends to become very long. When $\omega_{\mathrm{pm}}/\omega_{\mathrm{pe}} = 1$, L_{ENL} is always equivalent to the magnetic nonlinear length L_{HNL}. Second, when $\omega_{\mathrm{pm}}/\omega_{\mathrm{pe}} > 1$, or $\omega_{\mathrm{pm}}/\omega_{\mathrm{pe}} < 1$, both the diffraction length L_{DF} and the dispersion length L_{DS} near the plasma frequency become very short. Finally, and most importantly, the four characteristic lengths for describing the pulse propagation are dependent not only on the parameters of the electromagnetic pulse itself but also on the electric and magnetic plasma frequencies related to the sizes of split-ring resonators and wires for MMs. As a result, we can engineer the magnitude for these four lengths by adjusting the structural sizes of the MMs. These provide us with an alternative approach to manipulating electromagnetic pulse evolution not accessible in natural media

III. PROPAGATION PROPERTIES OF SPATIOTEMPORAL ELECTROMAGNETIC PULSES IN METAMATERIALS

A. Spatiotemporal electromagnetic solitons in metamaterials

Now, let us concentrate on Eq. (5) again. Apparently, it is formally identical to that for light pulse propagation in conventional materials except for the diffraction term. As a result, when we only consider the temporal pulse propagation in MMs, the conditions for the bright and dark

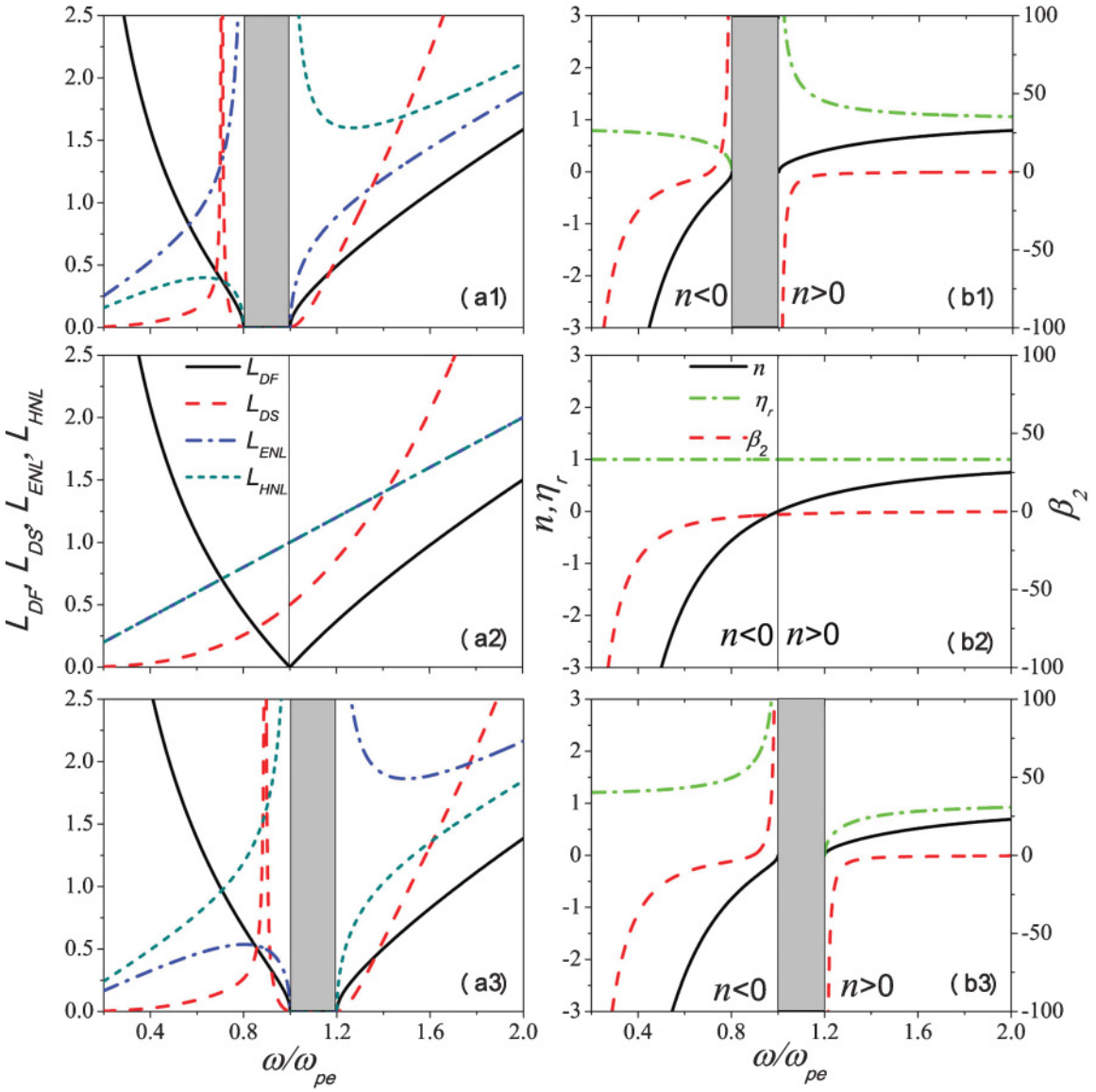

FIG. 1. (Color online) The four characteristic lengths L_{DF}, L_{DS}, L_{ENL}, and L_{HNL} (left) and n, η_r, and β_2 (right) versus normalized frequency $\omega/\omega_{\mathrm{pe}}$ for $\omega_{\mathrm{pm}}/\omega_{\mathrm{pe}}$= 0.8 (first row), 1.0 (second row), and 1.2 (third row), respectively. Here L_{DF}, L_{DS}, L_{ENL}, and L_{HNL} are calculated in units of L^0_{DF}, L^0_{DS}, L^0_{ENL}, and L^0_{HNL}, respectively, and β_2 is calculated in units of $1/c\omega_{\mathrm{pe}}$.

soliton formation are the same as those in conventional materials, irrespective of the sign of the refractive index [27]. However, when we consider the combined effects of dispersion, diffraction, and nonlinearity, the dynamics of the three-dimensional spatiotemporal soliton will become richer and more interesting owing to the fact that the sign of diffraction has an alternate choice of being negative, compared to that in conventional material where the sign of diffraction is always positive. Based on the well-known results drawn from the NLSE for light pulse propagation in conventional media [1–3,35], we note that, for $\mathrm{sgn}\,(\beta_2)\ \mathrm{sgn}\,(n) < 0$ and $s = 1$, Eq. (5) exhibits complete symmetry between time and space variables. As a consequence, for the positive-index region of MMs, spatiotemporal electromagnetic solitons may only form in focusing nonlinear materials with anomalous GVD; while for the negative-index region of MMs, spatiotemporal electromagnetic solitons can form even in defocusing nonlinear material with normal GVD. Such counterintuitive conditions obtained can be easily understood by noting that the role of diffraction is equivalent to that of anomalous dispersion in the positive-index region, whereas diffraction plays the role of normal dispersion in the negative-index region of MMs due to negative refraction. This leads to the fact that self-defocusing nonlinearity acts in opposition not only to normal dispersion but also to anomalous diffraction. As a result, it is conceivable that a suitable defocusing nonlinearity can delicately balance both normal dispersion and diffraction simultaneously, resulting in spatiotemporal electromagnetic soliton formation in MMs.

To better understand these results, here we borrow the analytical solutions to the NLSE for conventional media derived from the variational approach to further analyze the existence of a spatiotemporal electromagnetic soliton and the characteristics of its evolution in MMs. We assume the

envelope of the electric field of the pulse in MMs retains a Gaussian shape along the temporal and transverse spatial directions and is written as

$$A(X,Y,T,Z) = a\exp\left[-\frac{X^2+Y^2+T^2}{2w^2}\right] \times \exp[ib(X^2+Y^2+T^2)+i\phi], \quad (11)$$

where the self-similar evolution of the beam is parametrized by the Z-dependent amplitude $a(Z)$, spatiotemporal radius $w(Z)$, wave-front curvature $b(Z)$, and phase $\phi(Z)$. Using the variational approach [35,36] and skipping the straightforward details of the calculations, we present the following set of conventional differential equations to govern the evolution of parameters of ansatz (12):

$$\frac{d^2w}{dZ^2} = \frac{1}{w^3} - \mathrm{sgn}(n)\frac{I_0 p}{2\sqrt{2}w^4}, \quad (12a)$$

$$b = \frac{\mathrm{sgn}(n)}{2w}\frac{dw}{dZ}, \quad (12b)$$

$$\frac{d\phi}{dZ} = -\mathrm{sgn}(n)\frac{3}{2w^2} + \frac{7I_0 p}{8\sqrt{2}w^3}, \quad (12c)$$

where $I_0 = a^2w^3$ is the "energy" which is conserved during the pulse evolution. When Eq. (12a) is integrated once, we easily obtain the potential-well description:

$$\frac{1}{2}\left(\frac{dw}{dZ}\right)^2 + V(w) = 0, \quad (13)$$

where the potential V is

$$V(w) = \frac{1}{2w^2} - \mathrm{sgn}(n)\frac{I_0 p}{6\sqrt{2}w^3} + \mathrm{sgn}(n)\frac{I_0 p}{6\sqrt{2}} - \frac{1}{2}. \quad (14)$$

Here, the initial curvature $b(0) = 0$ and the initial spatiotemporal radius $w(0) = 1$ are assumed. Note that we do not specify the sign of n in deriving Eqs. (12)–(14), so they are formally applied to both conventional materials and MMs. It is easy to infer from Eqs. (12)–(14) that a spatiotemporal soliton may be excited when $\mathrm{sgn}(n)\,\mathrm{sgn}(p) = 1$ while an electromagnetic pulse always spreads along the temporal and spatial directions when $\mathrm{sgn}(n)\,\mathrm{sgn}(p) = -1$. In addition, we find that the phase and the wave-front curvature of the soliton are negative in the negative-index region of MMs, while they are positive in the positive-index region. In particular, it is worth noting that, although Eqs. (13) and (14) obtained by a variational approach are approximate, they just resemble the equations describing the dynamics of a particle in a one-dimensional potential well. As a result, using this analogy we can acquire a deeper physical understanding of the dynamics of electromagnetic pulse in MMs. In Fig. 2(a) we plot the potential V as a function of spatiotemporal radius w for different values of $I_0|p|$, and Fig. 2(b) illustrates the corresponding spatiotemporal radius w as a function of propagation distance Z. These results presented by the variational approach clearly show that the electromagnetic pulse will undergo diffraction ($I_0|p| < 2\sqrt{2}$), become a spatiotemporal electromagnetic soliton ($I_0|p| = 2\sqrt{2}$), or collapse ($I_0|p| > 2\sqrt{2}$), depending on competitions among the effects of nonlinearity and GVD together with diffraction. In addition, we find that, since the potential well cannot be created, as shown in Fig. 2(a), such

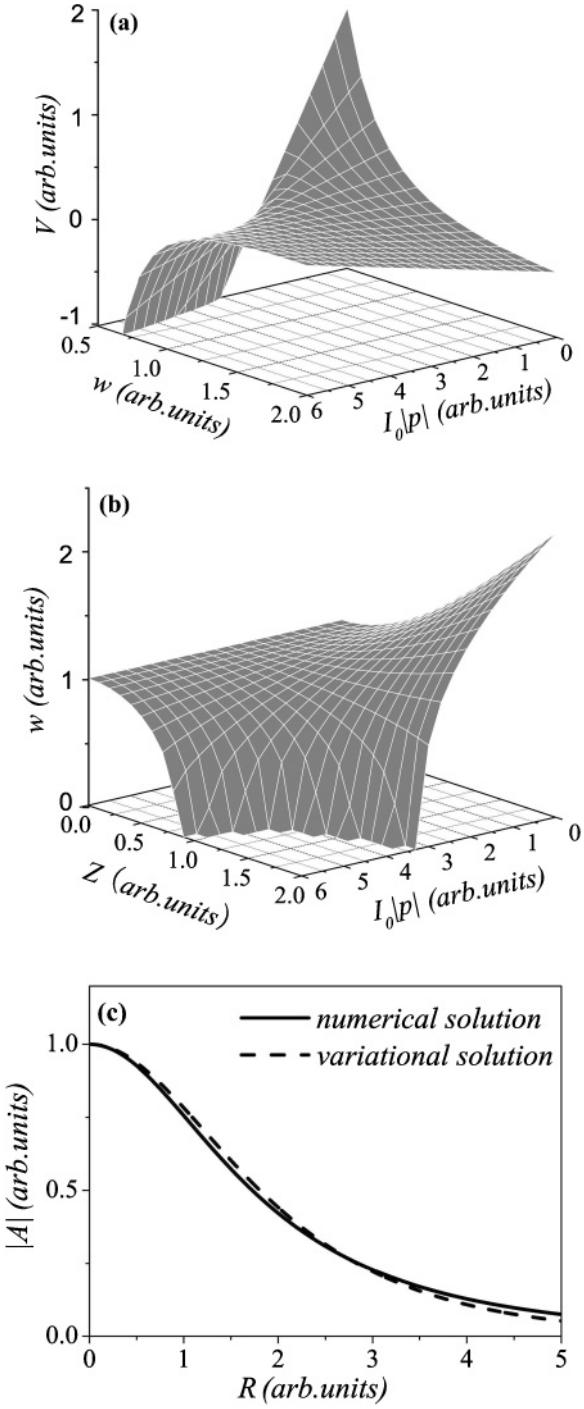

FIG. 2. Spatiotemporal electromagnetic soliton formation in the defocusing MMs with normal dispersion or in the focusing MMs with anomalous dispersion. (a) Qualitative plot of the potential function V as the function of spatiotemporal radius w for different values of $I_0|p|$. (b) Spatiotemporal radius w as the function of propagation distance Z for different values of $I_0|p|$. (c) Comparison of the radial profiles of spatiotemporal electromagnetic solitons for variational and numerical solutions; the field is normalized to unity at $R = 0$.

an equilibrium solution in MMs with simultaneous cubic electric and magnetic nonlinearity is unstable, and even a small deviation from the ideal self-trapped solution will lead to either divergence or collapse simultaneously along temporal

and spatial directions. Further, we make the substitution $A \to \sqrt{|p|}A$ in Eq. (5) and numerically solve it by using Runge-Kutta arithmetic in the spherical symmetric coordinate $R = \sqrt{X^2 + Y^2 + T^2}$ [3,35]. Figure 2(c) shows that the radial field profile of the approximate solution predicted by the variational approach agrees quite well with the exact numerical solution.

For the creation of spatiotemporal electromagnetic solitons in optical media, the ultimate goal of experimental and theoretical arrangements is to achieve a delicate balance among nonlinearity, diffraction, and dispersion. Therefore, the search for a material with suitable dispersion, diffraction, and nonlinearity is of the greatest importance. As is well known, for typical experimental parameters in conventional materials, one of the great challenges for realizing spatiotemporal electromagnetic solitons is that diffraction usually is stronger than dispersion (i.e., $s \ll 1$) [1–4]. The MMs, however, may completely overcome this limitation. As shown in Fig. 1, large GVD can be produced so that the dispersion effect can be comparable to the diffraction effect in this situation, meaning that we can facilitate matching of diffraction and dispersion (i.e., $s = 1$). For instance, we clearly see that, for $\omega_0/\omega_{pe} = 0.728$ or $\omega_0/\omega_{pe} = 1.169$ in the case of $\omega_{pm}/\omega_{pe} = 0.8$, spatiotemporal electromagnetic solitons can be excited in both positive- and negative-refractive index regions by adjusting the strength of nonlinearity. Most importantly, the lengths for dispersion, diffraction, and electric and magnetic nonlinearity are dependent on the structural parameters of MMs, indicating that we can engineer the balance among them by adjusting the sizes of the typical constitutive elements of MMs. As a result, compared with conventional materials, MMs can be designed to have more desirable linear and nonlinear electromagnetic responses for creating spatiotemporal electromagnetic solitons; thus they will become a promising candidate for generating and manipulating multidimensional solitons.

B. Spatial ring formation of electromagnetic pulses in metamaterials

In this section, we will unfold an interesting pulse propagation phenomenon associated with the negative refractive index of the MM, that is, the spatial ring formation of an electromagnetic pulse in the MM. The symmetry between time and space in Eq. (5) shows, when refractive index, dispersion, and nonlinearity meet the conditions $\mathrm{sgn}(\beta_2)\,\mathrm{sgn}(p) < 0$ and $\mathrm{sgn}(n)\,\mathrm{sgn}(p) < 0$, we can deduce that a spatial splitting of the pulse will occur in the optical media; especially for a circular beam, a spatial ring formation may appear in the transverse spatial direction. In conventional materials, because $\mathrm{sgn}(n) > 0$, a light pulse will undergo spatial splitting for $\mathrm{sgn}(\beta_2) > 0$ and $\mathrm{sgn}(p) < 0$, namely, in defocusing nonlinear materials with normal GVD. Similar phenomena have been reported in saturating nonlinear optical media [7]. However, for the negative-index region of MMs, due to $\mathrm{sgn}(n) < 0$, a spatial ring formation of an electromagnetic pulse may take place for $\mathrm{sgn}(\beta_2) < 0$ and $\mathrm{sgn}(p) > 0$, namely, in focusing nonlinear materials with anomalous GVD. In order to get better insight into the physical mechanism for the spatial ring formation of the pulse in the negative-index region of MMs, we will have to solve Eq. (5) by employing the split-step Fourier method, inasmuch as it has no analytic solution in this situation. Here, it is assumed that the initial envelope of the electric field of the pulse retains a Gaussian shape along temporal and spatial directions and is written as

$$A(X, Y, T, Z = 0) = \exp\left(-\frac{X^2 + Y^2 + T^2}{2}\right). \quad (15)$$

We summarize the typical evolutions of the pulse in Fig. 3. Figures 3(a) and 3(b) show the space-time profile and ring formation at $Z = 0.1L_{DF}$, respectively, and the corresponding detailed evolutions for temporal and spatial profiles with propagation distance are illustrated in Figs. 3(c) and 3(d), respectively. In the numerical simulations, we set $\omega_0/\omega_{pe} = 0.632$, $L^0_{DF} = 24L^0_{ENL}$, and $\mathrm{sgn}(\chi^{(3)}_m) = \mathrm{sgn}(\chi^{(3)}_p) = 1$, which correspond to $s = 3.0$ and $p = 50.5$ for $\omega_{pm}/\omega_{pe} = 0.8$. We choose the parameters for the purpose of satisfying the condition for spatial splitting of the pulse to occur, that is, $s > 1$ (to be given in the following), $\mathrm{sgn}(\beta_2) < 0$, and $\mathrm{sgn}(p) > 0$. The results observed in Fig. 3 clearly show that the peak intensity first increases, then decreases with increasing propagation distance. In particular, at the position of the maximum peak intensity, pulse splitting along the spatial direction begins to appear. In addition, we find that the compression in the temporal domain can be prevented by the spatial splitting at relatively larger propagation distance. Obviously, such an evolution for an electromagnetic pulse in the negative-index region of the MM is quite different from its counterpart in conventional materials under the same condition [3]. From a simple physical standpoint, we can understand the anomalous phenomena of electromagnetic pulse evolution as follows. It is well known that both focusing nonlinearity-induced self-phase modulation (SPM) and anomalous dispersion together act to compress the pulse, yet the effect of anomalous diffraction interacting with focusing nonlinearity always brings about beam spreading in MMs. As a result, when dispersion is stronger than diffraction (i.e., $s > 1$), under the action of strong enough SPM the electromagnetic pulse is initially compressed along the temporal direction faster than the spreading along the spatial direction, resulting in a rapid increase of the peak intensity. Subsequently, the spatial focusing nonlinearity will become relatively important with peak intensity increasing, so that the combined action of spatial focusing nonlinearity and diffraction makes the electromagnetic pulse spatial splitting occur, resulting in the spatial ring formation.

C. Temporal splitting of electromagnetic pulses in metamaterials

As is well known, temporal splitting of light pulses in conventional materials may occur for focusing nonlinearity and normal GVD [5,6]. In MMs, however, the condition is changed in the negative-index region. The symmetry between space and time in Eq. (5) shows that the signs of nonlinearity and dispersion will be reversed due to the negative index of refraction in the negative-index region of MMs. Typical evolutions of electromagnetic pulses in the defocusing MM with anomalous GVD are summarized in Fig. 4 by solving numerically Eq. (5). Figure 4(a) shows the space-time profile at $Z = 1.15L_{DF}$, and Figs. 4(b) and 4(c) illustrate the corresponding evolutions of temporal and spatial profiles with propagation

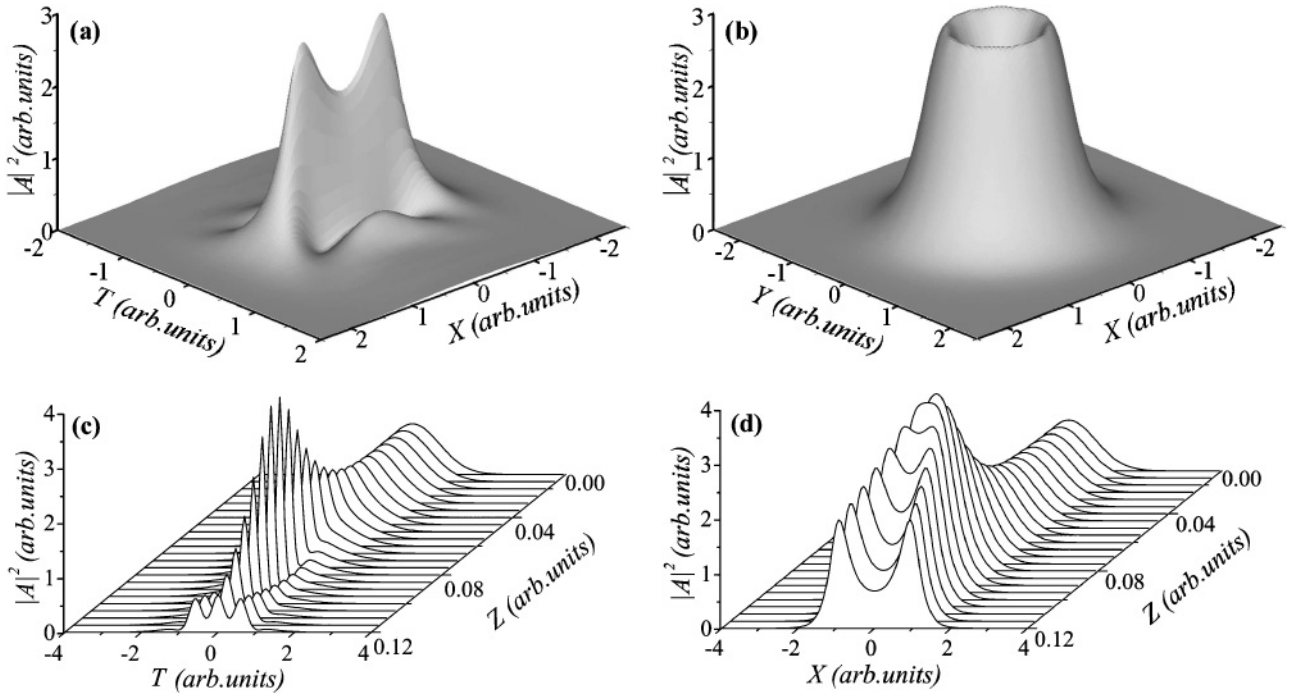

FIG. 3. Spatial ring formation of an electromagnetic pulse in focusing MMs with anomalous GVD. (a) Space-time profile ($Y = 0$). (b) Spatial ring formation ($T = 0$) at $Z = 0.1L_{\mathrm{DF}}$. (c) Evolution of on-axis temporal profile ($X = Y = 0$) as a function of propagation distance Z. (d) Evolution of on-axis spatial profile ($Y = T = 0$) as a function of propagation distance Z.

distance, respectively. To obtain typical results, the parameter values for the simulations are taken as $\omega_0/\omega_{\mathrm{pe}} = 0.699$, $L^0_{\mathrm{DF}} = 2.5L^0_{\mathrm{ENL}}$, and $\mathrm{sgn}\,(\chi_m^{(3)}) = \mathrm{sgn}\,(\chi_p^{(3)}) = -1$, which correspond to $s = 0.33$ and $p = -3.39$ for $\omega_{\mathrm{pm}}/\omega_{\mathrm{pe}} = 0.8$. From the results in Fig. 4, for the case of defocusing nonlinearity and anomalous GVD, the temporal splitting of the electromagnetic pulse is clearly observed in the negative-index region of MMs during the propagation, while the light pulse in conventional materials will always spread along temporal and spatial directions under the same conditions. Here, we present some qualitative explanation of the underlying physics as follows. Both defocusing nonlinearity-induced SPM and anomalous dispersion act to lead to a monotonic pulse spreading; however, the interaction of negative diffraction and defocusing nonlinearity tends to compress the beam in MMs. As a result, when diffraction is stronger than dispersion (i.e., $s < 1$), the strong enough self-defocusing nonlinearity can initially move energy toward the peak of the pulse from the off-axis spatial field faster than the anomalous dispersion can move it to the off-axis temporal field, thus leading to a rapid increase of peak intensity. As the peak intensity continues to increase, the impact of SPM on the pulse evolution will become more pronounced. As a result, at a relatively larger propagation distance the combination of SPM and GVD will be enough to push the energy away from $T = 0$, initiating the pulse splitting along the temporal direction, As this process continues, the peak intensity drops, and stops the spatial collapse.

D. The switchable sign of nonlinearity and its role in the propagation of electromagnetic pulses in metamaterials

Finally, let us analyze the switchable sign of the nonlinear term in Eq. (5) by adjusting the structural parameters of the MM and its role in the propagation of electromagnetic pulses. As Eq. (6) shows, the sign of the nonlinearity parameter p is determined by the combined effect of electric susceptibility $\chi_p^{(3)}$ and magnetic susceptibility $\chi_m^{(3)}$. In particular, for $\chi_p^{(3)}$ and $\chi_m^{(3)}$ having different signs [i.e., $\mathrm{sgn}\,(\chi_m^{(3)}/\chi_p^{(3)}) = -1$], the sign of p can be engineered by varying the ratio between the electric and magnetic plasma frequencies. For $\mathrm{sgn}\,(\chi_p^{(3)}) = -1$ and $\mathrm{sgn}\,(\chi_m^{(3)}) = 1$, if $\omega_{\mathrm{pm}}/\omega_{\mathrm{pe}} > 1$ and $\mathrm{sgn}\,(n) < 0$, or if $\omega_{\mathrm{pm}}/\omega_{\mathrm{pe}} < 1$ and $\mathrm{sgn}\,(n) > 0$, the MM will exhibits defocusing nonlinear characteristics ($p < 0$), while if $\omega_{\mathrm{pm}}/\omega_{\mathrm{pe}} < 1$ and $\mathrm{sgn}\,(n) < 0$, or if $\omega_{\mathrm{pm}}/\omega_{\mathrm{pe}} > 1$ and $\mathrm{sgn}\,(n) > 0$, the MM will exhibit focusing nonlinear characteristics ($p > 0$). For $\mathrm{sgn}\,(\chi_p^{(3)}) = 1$ and $\mathrm{sgn}\,(\chi_m^{(3)}) = -1$, the opposite situation will occur. As a consequence, due to the switchable sign of nonlinearity, the propagation of the electromagnetic pulse in the MM will become much richer and more interesting. For instance, according to the preceding discussions, if $\mathrm{sgn}\,(\chi_p^{(3)}) = -1$ and $\mathrm{sgn}\,(\chi_m^{(3)}) = 1$, the spatial ring formation and temporal splitting of the electromagnetic pulse may occur for $\omega_{\mathrm{pm}}/\omega_{\mathrm{pe}} < 1$ and $\omega_{\mathrm{pm}}/\omega_{\mathrm{pe}} > 1$, respectively, for $\mathrm{sgn}\,(n) < 0$. In the opposite situation [i.e., $\mathrm{sgn}\,(\chi_p^{(3)}) = 1$ and $\mathrm{sgn}\,(\chi_m^{(3)}) = -1$], the spatial ring formation and temporal splitting of the electromagnetic pulse may occur for $\omega_{\mathrm{pm}}/\omega_{\mathrm{pe}} > 1$ and $\omega_{\mathrm{pm}}/\omega_{\mathrm{pe}} < 1$, respectively, for $\mathrm{sgn}\,(n) < 0$. On the other hand, spatiotemporal electromagnetic solitons can be excited in both positive-index and negative-index regions. For $\mathrm{sgn}\,(\chi_p^{(3)}) = -1$ and $\mathrm{sgn}\,(\chi_m^{(3)}) = 1$, a spatiotemporal electromagnetic soliton can form when $\omega_{\mathrm{pm}}/\omega_{\mathrm{pe}} > 1$, while for $\mathrm{sgn}\,(\chi_p^{(3)}) = 1$ and $\mathrm{sgn}\,(\chi_m^{(3)}) = -1$, it can only appear when $\omega_{\mathrm{pm}}/\omega_{\mathrm{pe}} < 1$. To sum up, we can conclude that, when the sign of the normalized nonlinear parameter p satisfies the corresponding conditions given here by adjusting the structural parameters of

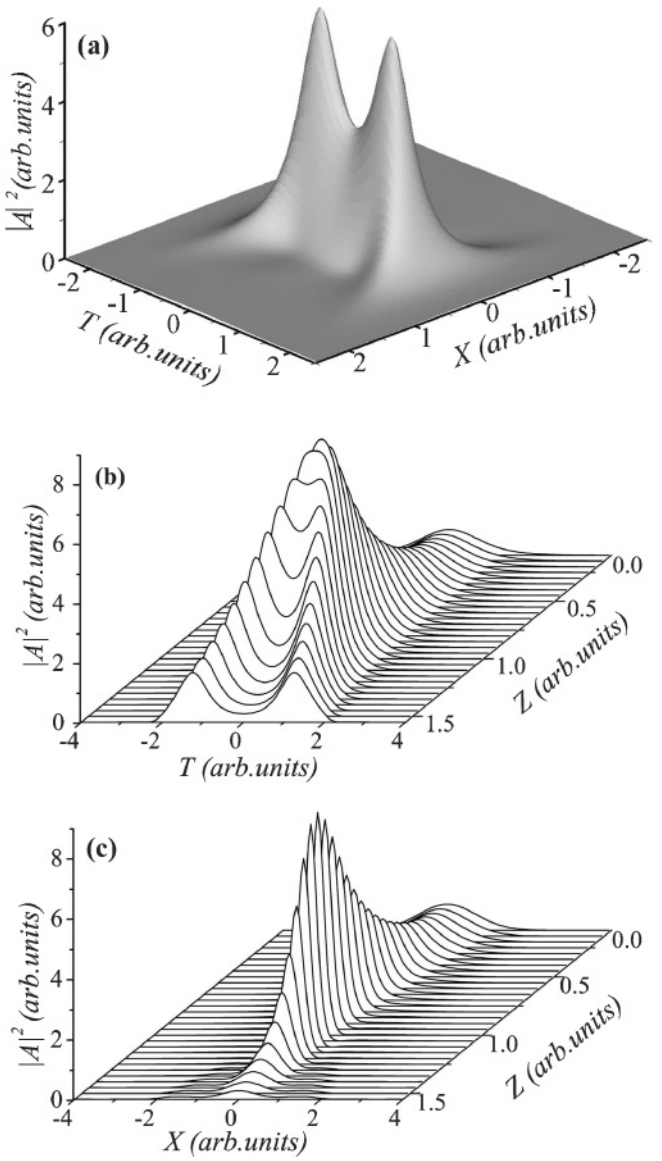

FIG. 4. Temporal splitting of an electromagnetic pulse in defocusing MMs with anomalous GVD. (a) Space-time profile ($Y = 0$) at $Z = 1.15L_{\mathrm{DF}}$. (b) Evolution of on-axis temporal profile ($X = Y = 0$) as a function of propagation distance Z. (c) Evolution of on-axis spatial profile ($Y = T = 0$) as a function of propagation distance Z.

MMs, a spatiotemporal electromagnetic soliton, a spatial ring, and temporal splitting of the electromagnetic pulse can occur regardless of the individual signs of the electric and magnetic nonlinearity. The switchable sign of the nonlinearity allows us to manipulate the dynamical behaviors of electromagnetic pulses in MMs more freely.

IV. CONCLUSIONS

In this paper, we provide a comprehensive investigation of the nonlinear dynamics of spatiotemporal electromagnetic pulses in MMs with simultaneous cubic electric and magnetic nonlinearity. Referring to the theoretical analysis of the pulsed beam propagation in conventional nonlinear optics, we try to disclose some unusual propagation properties of the spatiotemporal pulses associated with the unique electromagnetic properties of MMs, and we discuss the manipulation of the dynamical behaviors of electromagnetic pulses in MMs. We predict the existence of spatiotemporal electromagnetic solitons not only for the case of focusing nonlinearity with anomalous dispersion but also for the case of defocusing nonlinearity with normal dispersion. Especially, it is found that MMs can be exploited to create appropriate experimental circumstances for generating and manipulating spatiotemporal electromagnetic solitons. In addition, we demonstrate that spatial ring formation and temporal splitting of electromagnetic pulses may occur for the case of focusing and defocusing nonlinearity with anomalous dispersion, respectively. Finally, we find that the sign of nonlinearity for MMs can be engineered by varying the ratio between the electric and magnetic plasma frequencies, allowing us to manipulate the dynamical behaviors of electromagnetic pulses in MMs more freely. We hope that our findings will be helpful in manipulating electromagnetic pulse at will through the controllable linear and nonlinear properties of MMs and in stimulating further investigations on the nonlinear interaction of ultrashort electromagnetic pulses with MMs.

ACKNOWLEDGMENTS

This work was supported by the National Natural Science Foundation of China (Grants No. 10974049 and No. 60890202).

[1] For a review, see, for example, B. A. Malomed, D. Mihalache, F. Wise, and L. Torner, J. Opt. B: Quantum Semiclassical Opt. **7**, R53 (2005).
[2] Y. S. Kivshar and G. P. Agrawal, *Optical Solitons: From Fibers to Photonic Crystals* (Academic Press, San Diego, 2003).
[3] Y. Silberberg, Opt. Lett. **15**, 1282 (1990).
[4] L. Torner and Y. V. Kartashov, Opt. Lett. **34**, 1129 (2009).
[5] J. K. Ranka, R. W. Schirmer, and A. L. Gaeta, Phys. Rev. Lett. **77**, 3783 (1996).
[6] J. E. Rothenberg, Opt. Lett. **17**, 583 (1992).
[7] V. Skarka, V. I. Berezhiani, and R. Miklaszewski, Phys. Rev. E **60**, 7622 (1999).
[8] V. G. Veselago, Sov. Phys. Usp. **10**, 509 (1968).
[9] J. B. Pendry, D. Shurig, and S. R. Smith, Science **312**, 1780 (2006).
[10] J. B. Pendry, Phys. Rev. Lett. **85**, 3966 (2000).
[11] D. R. Smith, W. J. Padilla, D. C. Vier, S. C. Nemat-Nasser, and S. Schultz, Phys. Rev. Lett. **84**, 4184 (2000).
[12] V. M. Shalaev, W. Cai, U. K. Chettiar, H. Yuan, A. K. Sarychev, V. P. Drachev, and A. V. Kildishev, Opt. Lett. **30**, 3356 (2005).
[13] V. M. Shalaev, Nature Photonics **1**, 41 (2007).
[14] G. Dolling, C. Enkrich, M. Wegener, C. M. Soukoulis, and S. Linden, Opt. Lett. **31**, 1800 (2006).

[15] A. A. Zharov, I. V. Shadrivov, and Y. S. Kivshar, Phys. Rev. Lett. **91**, 037401 (2003).
[16] S. O'Brien, D. McPeake, S. A. Ramakrishna, and J. B. Pendry, Phys. Rev. B **69**, 241101(R) (2004).
[17] M. Lapine, M. Gorkunov, and K. H. Ringhofer, Phys. Rev. E **67**, 065601(R) (2003).
[18] N. Lazarides and G. P. Tsironis, Phys. Rev. E **71**, 036614 (2005).
[19] M. Scalora, M. S. Syrchin, N. Akozbek, E. Y. Poliakov, G. D'Aguanno, N. Mattiucci, M. J. Bloemer, and A. M. Zheltikov, Phys. Rev. Lett. **95**, 013902 (2005).
[20] S. Wen, Y. Xiang, X. Dai, Z. Tang, W. Su, and D. Fan, Phys. Rev. A **75**, 033815 (2007).
[21] A. Maluckov, Lj. Hadžievski, N. Lazarides, and G. P. Tsironis, Phys. Rev. E **77**, 046607 (2008).
[22] P. Tassin, L. Gelens, J. Danckaet, I. Veretennicoff, G. V. der Sande, P. Kockaert, and M. Tlidi, Chaos **17**, 037116 (2007).
[23] S. Wen, Y. Xiang, W. Su, Y. Hu, X. Fu, and D. Fan, Opt. Express **14**, 1568 (2006).
[24] Y. Xiang, S. Wen, X. Dai, Z. Tang, W. Su, and D. Fan, J. Opt. Soc. Am. B **24**, 3058 (2007).
[25] S. Wen, Y. Wang, W. Su, Y. Xiang, X. Fu, and D. Fan, Phys. Rev. E **73**, 036617 (2006).
[26] G. D'Aguanno, N. Mattiucci, M. Scalora, and M. J. Bloemer, Phys. Rev. Lett. **93**, 213902 (2004).
[27] G. D'Aguanno, N. Mattiucci, and M. J. Bloemer, J. Opt. Soc. Am. B **25**, 1236 (2008).
[28] N. L. Tsitsas, N. Rompotis, I. Kourakis, P. G. Kevrekidis, and D. J. Frantzeskakis, Phys. Rev. E **79**, 037601 (2009).
[29] M. Marklund, P. K. Shukla, and L. Stenflo, Phys. Rev. E **73**, 037601 (2006).
[30] P. P. Banerjee and G. Nehmetallah, J. Opt. Soc. Am. B **24**, A69 (2006).
[31] I. V. Shadrivov, A. A. Sukhorukov, Y. S. Kivshar, A. A. Zharov, A. D. Boardman, and P. Egan, Phys. Rev. E **69**, 016617 (2004).
[32] I. V. Shadrivov and Y. S. Kivshar, J. Opt. A: Pure Appl. Opt. **7**, S68 (2005).
[33] N. A. Zharova, I. V. Shadrivov, A. A. Zharov, and Y. S. Kivshar, Opt. Express **13**, 1291 (2005).
[34] Y. Liu, G. Bartal, D. A. Genov, and X. Zhang, Phys. Rev. Lett. **99**, 153901 (2007).
[35] M. Desaix, D. Anderson, and M. Lisak, J. Opt. Soc. Am. B **8**, 2082 (1991).
[36] D. Anderson, Phys. Rev. A **27**, 3135 (1983).